DOI: 10.1002/ejic.200600788

Constructing Multimetallic Systems with the Naphthalene-1,8-bis(thiolato) Ligand

Stuart D. Robertson,[a] Alexandra M. Z. Slawin,[a] and J. Derek Woollins*[a]

Keywords: Sulfur ligand / Multimetallic systems / Gold / Bridging ligands / X-ray structure

Addition of 1 equiv. $(Ph_3P)Au(ClO_4)$ (formed by ion exchange of Ph_3PAuCl with $AgClO_4$) to [naphthalene-1,8-bis(thiolato)]-bis(triphenylphosphane)platinum results in the formation of a novel dimetallic cationic complex with a (triphenylphosphane)gold moiety attached to the sulfur of the naphthalene-1,8-bis(thiolato) ligand. NMR spectroscopic evidence suggests that this gold-containing fragment is fluxional in its bonding and X-ray crystallography confirms the asymmetric complex, which shows this gold atom attached to one of these sulfur atoms. Addition of more than 1 equiv. $(Ph_3P)Au(ClO_4)$ results in the formation of a tetrametallic sandwich complex with two bridging gold atoms between the sulfur atoms of the two PtS_2C_3 rings. Tri- and tetrametallic silver-containing complexes can be prepared by addition of 0.5 and 1 equiv. $AgClO_4$ to $(Ph_3P)_2Pt(S_2C_{10}H_6)$, respectively.

Introduction

Heterometallic complexes formed by reaction of sulfur-containing platinum(II) complexes with a group 11 complex have been well documented recently and are of great interest as they have a variety of possibilities for coordination of the group 11 metal to the platinum complex. This can partly be attributed to the presence of sulfur in the platinum complex because gold and silver have a great affinity for sulfur. Any heterometallic complex formed by bonding of an Au or Ag complex to sulfur may or may not contain a Pt–M bond, depending on the geometry of the two metals around the sulfur centre. One of the most common starting materials is the highly nucleophilic complex $[\{Pt(PPh_3)_2(\mu\text{-}S)\}_2]$.[1] For example, the $AuPPh_3$ unit is inserted between the two sulfur atoms to give a trigonal-planar structure with no Pt···Au interaction.[2] Similarly, the analogous silver complex has also been obtained,[3] again with no interaction between the two metal atoms.

A number of complexes containing a gold(III) atom bridging the two sulfur atoms in a square-planar configuration have also been described recently.[4,5] These are formed by reaction of the platinum starting material with a gold(III) dichloride such as $Au(pap)Cl_2$ [pap = η^2 ligand, 2-(2-pyridylamino)phenyl]. The reaction of 2 equiv. $[Ag(PR_3)_2]^+$ with $[Pt(mnt)_2]^{2-}$ (mnt = maleonitriledithiolate, a bidentate S,S-bound ligand) also results in the insertion of silver between two sulfur atoms.[6] In this case, one Ag unit lies above the plane of the PtS_4 unit bound to two *cis* sulfur atoms, while the other lies between the other two sulfur atoms but below the plane.

Gold-containing species have also been treated with $[\{Pt(PPh_3)_2(\mu\text{-}S)\}_2]$ to give products where the gold fragment (Au–PPh_3) is bound to only one sulfur atom but not to the other so that it is not bridging.[7,8] Silver has also been seen bound to one or two sulfur atoms of ethylenedithiolato complexes in the form of $Ag(PPh_3)_2$.[9] This work has been extended so that both sulfur atoms bind to a different metal with no bridges between the two sulfur atoms, both in the gold[8,10] and silver complexes.[10,11]

While in all these examples the group 11 atom is in a configuration without Au/Ag···platinum interactions, examples are also known where an $MPPh_3$ fragment is bound to only one of the two platinum-bound sulfur atoms in a configuration with a Pt···M interaction.[12] In this case, the platinum starting material is not the butterfly-core-containing $[\{Pt(PPh_3)_2(\mu\text{-}S)\}_2]$ but is cyclometallated $[Pt\{CH_2C_6H_4P(C_6H_4Me\text{-}o)_2\}(S_2CNMe_2)]$.

While the previously mentioned examples have included complexes where one gold or silver atom is bridging between the two platinum-bound sulfur atoms, it is also possible for this bridge to contain two gold or silver atoms. For example, the hexametallic compound $[Au_2\{Pt_2(PPh_3)_4(\mu_3\text{-}S)_2\}_2]Cl_2$ is formed by reaction of 1 equiv. $[\{Pt(PPh_3)_2(\mu\text{-}S)\}_2]$ with 1 equiv. $AuCl(SMe_2)$.[10] This complex has a hexanuclear $\{Au_2Pt_4\}$ cage-framework comprising two hinged $\{Pt_2S_2\}$ groups anchored across an Au–Au bond as shown in Figure 1.

---

[a] School of Chemistry, University of St. Andrews,
Fife, Scotland, KY16 9ST, UK
Fax: +44-1334-463384
E-mail: jdw3@st-and.ac.uk

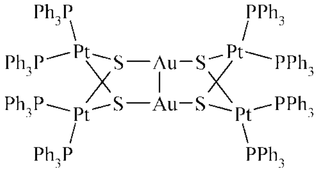

Figure 1. Structure of the dication of $[Au_2\{Pt_2(PPh_3)_4(\mu_3\text{-}S)_2\}_2]Cl_2$; the two anions are omitted for clarity.

Silver examples of this structure are also known, formed from $[\{Pt(PPh_3)_2(\mu\text{-}S)\}_2]$ and $AgBF_4$,[13] $AgNO_3$[13] and $AgClPPh_3$.[11] A similar complex exists where the two sulfur atoms share only a single platinum atom rather than two platinum atoms.[9] In each case, X-ray crystallographic data suggests that the two silver atoms are within bonding distance.

Examples are also known where two gold atoms attached to either sulfur atom are weakly bound or not bound to each other, but are connected through a larger phosphorus-containing backbone.[7] In this case, the starting materials are $[\{Pt(PPh_3)_2(\mu\text{-}S)\}_2]$ and either $Au_2Cl_2(dppm)$ or $Au_2Cl_2(dppf)$ [dppm = (diphenylphosphanyl)methane, dppf = (diphenylphosphanyl)ferrocene]. When the backbone is dppm, the two gold atoms are in close proximity (approximately 2.9 Å) such that a considerable aurophilic interaction can be considered to exist. In the case of dppf, the Au–Au distance is much larger [3.759(3) Å] and can be considered non-bonding.

We have a longstanding interest in the coordination and bridging effects of sulfur donor ligands.[14a,14b] Here, we report gold and silver complexes of $(Ph_3P_2)PtS_2C_{10}H_6$ where the sulfur atoms of one molecule of this complex are bridged to another molecule by either one or two group 11 atoms.

Results and Discussion

The anionic exchange of the gold complex Ph_3PAuCl with $AgClO_4$ proceeds smoothly in a mixture of dichloromethane and acetonitrile at room temperature. The product is freed of AgCl by removing all solvent and re-dissolving the desired product in dichloromethane before filtering. The resultant gold complex reacts with $(Ph_3P)_2Pt(S_2C_{10}H_6)$ to give the cationic complex $[(Ph_3P)_2Pt(S_2C_{10}H_6)(AuPPh_3)]^+$-$ClO_4^-$ (**1**).

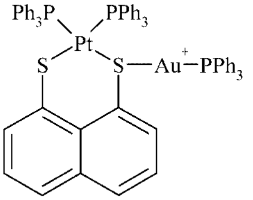

1

The ^{31}P NMR spectrum of **1** shows a peak at δ = 32.7 ppm corresponding to the triphenylphosphane group attached to the gold atom and a peak at δ = 17.6 ppm corresponding to the two triphenylphosphane groups bonded to the central platinum atom. The expected platinum satellites are also evident, with a coupling constant of 3080 Hz, [over 100 Hz higher in magnitude than that of the starting material].[13] The asymmetry of complex **1** caused by the gold-containing fragment bonded to one sulfur atom suggests that the two platinum-bound phosphorus atoms should be non-equivalent and therefore should display an AB spin system. However, fluxionality of this gold fragment from one sulfur atom to the other, as seen in Scheme 1, causes these two Pt-coordinated phosphane groups to appear equivalent down to temperatures as low as –80 °C, suggesting that this flipping from one sulfur atom to the other is relatively facile in solution.

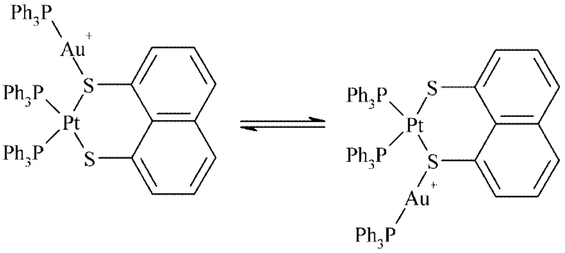

Scheme 1. The equilibrium in complex **1**. Perchlorate anion is omitted for clarity.

The ^{195}Pt NMR spectrum displays the expected peak at –4674 ppm with the corresponding phosphorus coupling. The mass spectrum (ES^+) of complex **1** shows the parent ion at *m/z* 1367–1370 in the predicted pattern with the primary peak at 1368. The identity of the counteranion is proved by the ES^- mass spectrum, which shows two peaks at 99 and 101 in the correct ratio.

Complex **2** is formed by the reaction of more than one equilavent of $Ph_3PAu^+ClO_4^-$ with $(Ph_3P)_2Pt(S_2C_{10}H_6)$ in dichloromethane. This tetrametallic dication is charge-balanced with two perchlorate ions.

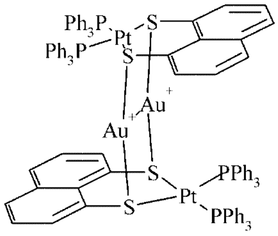

2

Complexes **3** and **4** are formed by addition of a solution containing 0.5 and 1 equiv. $AgClO_4$ (in acetronitile) to $(Ph_3P)_2Pt(S_2C_{10}H_6)$ (in tetrahydrofuran), respectively. It is somewhat surprising that we could not obtain a simple gold analogue of **3** [especially considering the lability of the Au–P bond in the formation of **2**], and this may reflect the very strong preference for linear geometry in Au^I; we did attempt to prepare gold complexes from $HAuCl_4$ but obtained intractable mixtures.

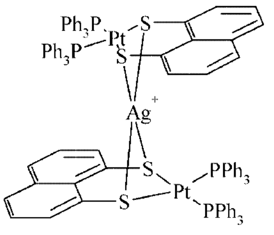

3

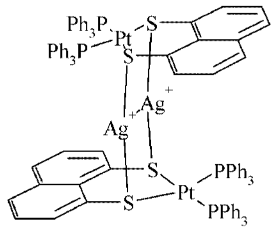

4

Isolation of the final complexes was achieved by removing the mixed solvent in vacuo, redissolving in a minimum volume of dichloromethane and precipitating by slow addition of diethyl ether while stirring. The final products are obtained as an orange and a yellow powder, respectively.

The ^{31}P NMR spectra of complexes **3** and **4** show a peak at δ = 6.8 and 18.3 ppm, respectively, with platinum satellites. The coupling constants for these sets of peaks are 2989 Hz (complex **3**) and 3122 Hz (complex **4**). This value for complex **4** is close to that of the digold analogue **2**. The ^{195}Pt NMR spectrum of **3** displays a triplet at –4698 ppm. Unfortunately, no peak was observed in the ^{195}Pt NMR spectrum of **4**, possibly because the sample was not sufficiently concentrated. The mass spectrum (ES$^+$) of complex **3** is excellent, displaying the parent ion at 1927–1932 in the predicted pattern with the primary peak at 1929. The mass spectrum of **4** displays the expected peaks in the region 1016–1019, half the mass of the complex, which is expected since this complex carries a 2+ charge. The identity of the counteranion in both cases is again proved by the ES$^-$ mass spectrum, which shows two peaks at 99 and 101 in the correct ratio.

X-ray Crystallography

The crystal structures of complexes **1**–**4** are shown in Figures 3–7, and selected bond lengths and angles are in Table 1 and Table 2. The crystal structure of $(Me_3P)_2Pt(S_2C_{10}H_6)$[15] is also shown (Figure 2 as this complex is closely related to the starting material $(Ph_3P)_2Pt(S_2C_{10}H_6)$, which has never been crystallographically characterised, and is useful for comparison with the complexes **1**–**4**. The X-ray analysis of complex **1** (see Figure 3 and Table 1) shows that the $AuPPh_3$ unit is attached to only one of the sulfur atoms, S(1)–Au(1) = 2.3614(12) and S(9)–Au(1) = 2.979(1) Å. These values, along with the virtually linear S(1)–Au(1)–P(3) angle [174.71(4)°] are similar to those of other disulfur complexes containing a Au–PPh$_3$ arm on one of the sulfur atoms[7,8] and longer than, for example, the Au–S distances in linear [RS–Au–SR]$^-$ containing anionic S donors.[15] The Au(1)–P(3) bond length is also similar to those seen previously. The addition of the Au–PPh$_3$ arm also changes the geometry around S(1) so that it is now in a distorted trigonal-planar structure. This distortion is proven since the largest of the three angles around this sulfur atom is only 104°, a significant deviation from perfect trigonal planarity (120°). This suggests that the geometry around this sulfur atom can possibly be considered as trigonal pyramidal. This new gold fragment considerably reduces the Pt–S(1)–C(1) angle by almost 10°. This forces the naphthalene backbone to realign slightly, which results in the dihedral angle [deviation form planarity between the Pt(1)–S(1)–S(9) and C(10)–S(1)–S(9) planes] being markedly reduced from 136° in $(Me_3P)_2Pt(S_2C_{10}H_6)$ to only 121°. The effect of the gold-containing arm on the geometry around the Pt atom is only slight, a 3° tightening of the S–Pt–S angle is noticed, which in turn is compensated for by a 4° widening of the P–Pt–P angle, resulting in a more distorted square-planar arrangement around the platinum centre with respect to the square-planar platinum complex $(Me_3P)_2Pt(S_2C_{10}H_6)$. This tightening of the S–Pt–S bond also results in a smaller splay angle (18.6°) in complex **1**, as expected. The changes in bond lengths relative to those in $(Me_3P)_2Pt(S_2C_{10}H_6)$ are negligible.

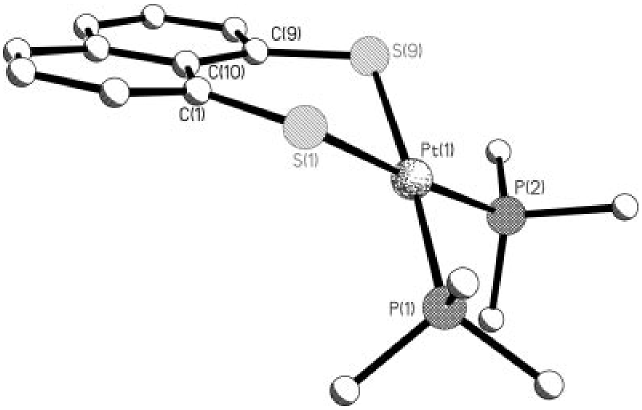

Figure 2. Crystal structure of $(Me_3P)_2Pt(S_2C_{10}H_6)$.[15] This complex is closely related to the starting material $(Ph_3P)_2Pt(S_2C_{10}H_6)$, which has never been crystallographically characterised, and is useful for a comparison with the complexes **1**–**4**.

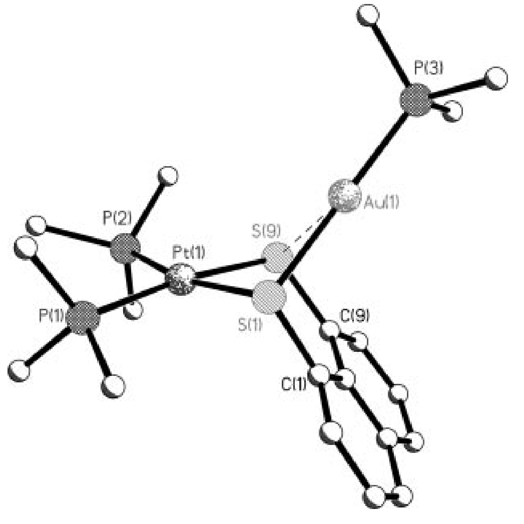

Figure 3. Crystal structure of $[(Ph_3P)_2Pt(S_2C_{10}H_6)(AuPPh_3)]^+ClO_4^-$ (**1**); ClO_4^- anion is omitted for clarity.

We found no intermolecular packing effects in the solid-state structure of **1**, which would account for the longer Pt–S(9) distance.

Table 1. Bond lengths [Å] and angles [°] for platinum starting material and complexes **1** and **3**, where M = Au (**1**) and Ag (**3**).

	$(Me_3P)_2Pt(S_2C_{10}H_6)$[15]	**1**	**3**
Pt(1)–S(1)	2.320(1)	2.3492(12)	2.352(4)
Pt(1)–S(9)	2.326(1)	2.3504(12)	2.362(4)
Pt(1)–P(1)	2.284(1)	2.3121(12)	2.319(4)
Pt(1)–P(2)	2.273(1)	2.2985(13)	2.307(4)
S(1)–C(1)	1.754(4)	1.787(5)	1.788(16)
S(9)–C(9)	1.760(4)	1.775(5)	1.773(17)
S(1)–S(9)	3.22(9)	3.151(2)	3.184(5)
S(1)–M(1)	–	2.3614(12)	2.622(4)
S(9)–M(1)	–	2.979(1)	2.580(4)
M(1)–P(3)	–	2.2553(13)	–
Pt(2)–S(51)	–	–	2.363(4)
Pt(2)–S(59)	–	–	2.352(4)
Pt(2)–P(3)	–	–	2.303(4)
Pt(2)–P(4)	–	–	2.297(4)
S(51)–C(51)	–	–	1.792(16)
S(59)–C(59)	–	–	1.790(15)
S(51)–S(59)	–	–	3.192(5)
S(51)–M(1)	–	–	2.537(4)
S(59)–M(1)	–	–	2.690(4)
M(1)-Pt(1)	–	–	3.0739(13)
M(1)-Pt(2)	–	–	3.2044(13)
S(1)–Pt(1)–S(9)	87.62(4)	84.20(4)	84.99(13)
P(1)–Pt(1)–P(2)	96.55(4)	101.03(4)	100.03(14)
P(1)–Pt(1)–S(1)	85.88(4)	92.53(4)	90.14(13)
P(2)–Pt(1)–S(9)	89.97(4)	82.78(4)	85.86(14)
P(1)–Pt(1)–S(9)	173.45(4)	172.60(4)	170.07(14)
P(2)–Pt(1)–S(1)	176.83(4)	165.88(4)	168.04(14)
Pt(1)–S(1)–C(1)	113.24(14)	103.85(16)	107.7(5)
Pt(1)–S(1)–M(1)	–	98.10(4)	76.13(12)
C(1)–S(1)–M(1)	–	104.04(16)	112.7(5)
C(9)–S(9)–Pt(1)	110.28(14)	107.01(16)	105.8(5)
Pt(1)–S(9)–M(1)	–	82.87(3)	76.79(11)
C(9)–S(9)–M(1)	–	–	111.3(6)
S(1)–C(1)–C(10)	128.4(3)	124.9(4)	124.8(11)
C(10)–C(9)–S(9)	127.1(3)	127.7(4)	128.8(12)
C(1)–C(10)–C(9)	125.8(3)	126.0(5)	126.3(14)
S(51)–Pt(2)–S(59)	–	–	85.20(13)
P(3)–Pt(2)–P(4)	–	–	99.21(13)
P(3)–Pt(2)–S(51)	–	–	84.06(13)
P(4)–Pt(2)–S(59)	–	–	91.53(13)
P(3)–Pt(2)–S(59)	–	–	168.23(13)
P(4)–Pt(2)–S(51)	–	–	176.73(14)
Pt(2)–S(51)–C(51)	–	–	103.4(5)
Pt(2)–S(51)–M(1)	–	–	81.60(11)
C(51)–S(51)–M(1)	–	–	109.5(5)
C(59)–S(59)–Pt(2)	–	–	106.4(5)
Pt(2)–S(59)–M(1)	–	–	78.60(11)
C(59)–S(59)–M(1)	–	–	107.7(5)
S(51)–C(51)–C(60)	–	–	129.6(12)
C(60)–C(59)–S(59)	–	–	126.8(15)
C(51)–C(60)–C(59)	–	–	124.7(15)
S(1)–M(1)–P(3)	–	174.71(4)	–
S(9)–M(1)–P(3)	–	113.97(4)	–
S(1)–M(1)–S(9)	–	71.26(4)	75.49(12)
S(51)–M(1)–S(59)	–	–	75.20(11)
S(1)–M(1)–S(51)	–	–	148.85(13)
S(9)–M(1)–S(59)	–	–	139.22(13)
S(1)–M(1)–S(59)	–	–	94.31(12)
S(9)–M(1)–S(51)	–	–	131.00(12)
Splay angle	21.3	18.6	19.9, 21.1
Dihedral angle	136	121	124, 122

Complex **3** consists of two $[P_2PtS_2]$ units connected by a single bridging silver atom connected to all four sulfur atoms (see Figure 4. Both $[P_2PtS_2]$ units are similarly affected by the introduction of a silver atom between the two sulfur atoms. It is notable that the Ag–S distance is longer in **3** than in **4** (vide infra) and other Pt_2Ag_2 systems.[9] The silver atom pulls the two sulfur atoms closer together, as shown by the tighter S–Pt–S and Pt–S–C angles and the reduced splay angles on the naphthalene-1,8-bis(thiolato) backbone. With regard to the geometry around platinum, the reduced S–Pt–S angle is again compensated for by an increase in the P–Pt–P angle, and the configuration around the platinum atom deviates from square planarity. Similarly to complex **1**, the effect of the silver atom is such that the geometry around all the sulfur atoms changes to distorted trigonal pyramidal, with the largest angle around sulfur [C(1)–S(1)–Ag(1) = 112.7(5)°] displaying that there is considerable deviation from trigonal planarity. The presence of the silver atom has also forced the naphthalene backbone and the triphenylphosphane groups closer together, as proven by the reduced dihedral angles in complex **3**. The silver atom can be considered four coordinate and can probably best be described as having a heavily distorted tetrahedral geometry. The metal–sulfur bonds are in the range 2.537(4)–2.690(4) Å. The S(1)–Ag–S(9) and S(51)–Ag–S(59) bond angles are approximately 75°, but the other S–Ag–S angles (i.e. those involving two sulfur atoms from opposite molecules) have a large range, which displays the deviation away from a tetrahedral geometry. The smallest of these angles is only 94.31(12)°, while the largest is 148.85(13)°.

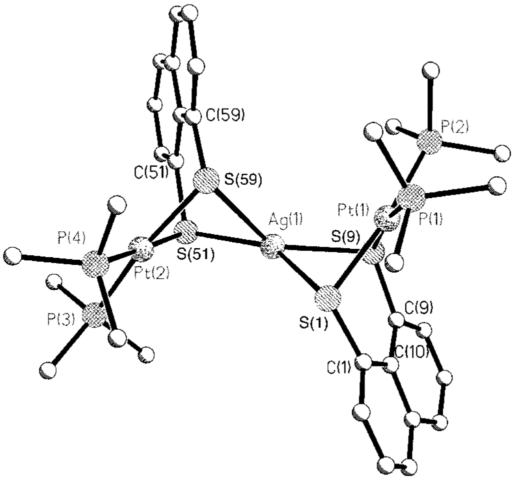

Figure 4. Crystal structure $Ag[(Ph_3P)_2Pt(S_2C_{10}H_6)]_2^+ClO_4^-$ (**3**); ClO_4^- anion is omitted for clarity.

Complex **2** was found to crystallise in two different unit cells, one monoclinic (Figure 5) and one triclinic (Figure 6). In each case, however, the bond lengths and angles are very similar (Table 2). Complex **4** gave a triclinic unit cell (Figure 7), and the structure is again similar to those obtained for **2**. In these structures, the two $[P_2PtS_2]$ units are linked to each other by two metal atoms as opposed to one metal atom in complex **3** such that there are two S–M–S bridges. The Au–S distances are shorter than the Ag–S distances as a consequence of the difference in the covalent radii of the metals. The distances reported here are comparable with those in ethylenethiolato Pt_2M_2 complexes, which also display similar $Pt_2M_2S_2$ six-membered chair conformation rings.[9] The bridging has a great effect on the geometry of the original platinum structures, although bond angles have changed by a negligible and unremarkable amount. While **3** was found to contain a six-membered MS_2C_3 ring, **2** and **4** contain seven-membered $M_2S_2C_3$ rings. This has had a converse affect as the insertion of the two new metal atoms actually increases the sulfur–sulfur distances and also the splay angles with respect to $(Me_3P)_2Pt(S_2C_{10}H_6)$. This results in the S–Pt–S angles widening slightly to almost exactly 90°. The P–Pt–P angles also increase slightly, but in this case, not as much as in complex **3**. This allows us to consider the platinum centre to be in a less distorted square-planar configuration than in $(Me_3P)_2Pt(S_2C_{10}H_6)$.

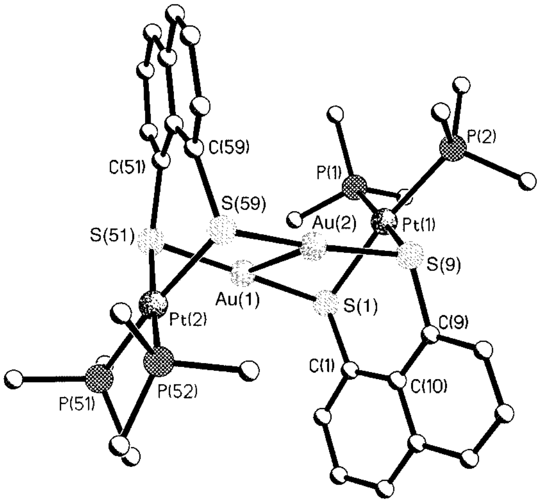

Figure 5. Crystal structure of $[Au(Ph_3P)_2Pt(S_2C_{10}H_6)]_2^{2+}2ClO_4^-$ (**2**); ClO_4^- anions are omitted for clarity.

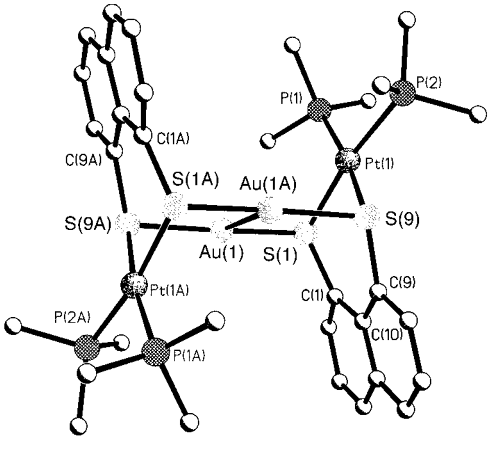

Figure 6. Crystal structure of $[Au(Ph_3P)_2Pt(S_2C_{10}H_6)]_2^{2+}2ClO_4^-$ (**2′**); ClO_4^- anions are omitted for clarity.

Again, the geometry around the sulfur atoms is trigonal pyramidal, but it is slightly closer to a trigonal planar geometry than that in **3** since the presence of the other metal atom pushes the metal atom closer to the plane of the S, C and Pt atoms. This is evidenced by a general increase in the bond angles around the sulfur atoms, moving towards 120°.

Table 2. Bond lengths [Å] and angles [°] for complexes **2** and **4**, where M = Au (**2**) and Ag (**4**).

	2	2′	4
Pt(1)–S(1)	2.3320(16)	2.318(4)	2.353(4)
Pt(1)–S(9)	2.3547(16)	2.344(4)	2.330(4)
Pt(1)–P(1)	2.2951(16)	2.299(4)	2.319(4)
Pt(1)–P(2)	2.3059(17)	2.297(4)	2.306(4)
S(1)–C(1)	1.801(6)	1.752(16)	1.774(16)
S(9)–C(9)	1.777(7)	1.783(14)	1.790(16)
S(1)–S(9)	3.315(2)	3.312(5)	3.356(7)
S(1)–M(1)	2.2943(16)	2.317(4)	2.426(5)
S(9)–M(1A)	–	2.327(4)	2.389(5)
S(9)–M(2)	2.3202(16)	–	–
M(1)–M(1A)	–	3.0042(14)	3.069(4)
Pt(2)–S(51)	2.3406(16)	–	–
Pt(2)–S(59)	2.3435(16)	–	–
Pt(2)–P(51)	2.3066(17)	–	–
Pt(2)–P(52)	2.2996(17)	–	–
S(51)–C(51)	1.810(7)	–	–
S(59)–C(59)	1.797(7)	–	–
S(51)–S(59)	3.336(2)	–	–
S(51)–M(1)	2.3069(16)	–	–
S(59)–M(2)	2.3174(16)	–	–
M(1)–M(2)	2.9801(4)	–	–
S(1)–Pt(1)–S(9)	90.02(6)	90.55(13)	91.54(15)
P(1)–Pt(1)–P(2)	96.39(6)	99.12(13)	98.88(15)
P(1)–Pt(1)–S(1)	90.08(6)	87.79(13)	83.15(15)
P(2)–Pt(1)–S(9)	84.04(6)	83.27(13)	87.13(15)
P(1)–Pt(1)–S(9)	174.24(6)	172.16(12)	171.53(14)
P(2)–Pt(1)–S(1)	171.88(6)	171.44(14)	173.46(14)
Pt(1)–S(1)–C(1)	115.0(2)	114.6(5)	118.7(6)
Pt(1)–S(1)–M(1)	98.25(6)	98.26(14)	89.84(15)
C(1)–S(1)–M(1)	106.3(2)	108.7(5)	109.4(5)
C(9)–S(9)–Pt(1)	110.1(2)	117.0(5)	114.1(6)
Pt(1)–S(9)–M(1A)	–	94.36(14)	95.98(17)
C(9)–S(9)–M(1A)	–	105.5(5)	112.0(5)
Pt(1)–S(9)–M(2)	100.84(6)	–	–
C(9)–S(9)–M(2)	108.4(2)	–	–
S(1)–C(1)–C(10)	129.0(5)	130.6(12)	126.2(13)
C(10)–C(9)–S(9)	126.6(5)	128.7(11)	129.6(13)
C(1)–C(10)–C(9)	126.8(6)	124.7(13)	126.9(15)
S(1)–M(1)–M(1A)	–	92.45(10)	94.47(14)
S(9A)–M(1)–M(1A)	–	95.10(10)	92.12(14)
S(1)–M(1)–S(9A)	–	171.92(14)	171.28(16)
S(1)–M(1)–M(2)	90.77(4)	–	–
S(51)–M(1)–M(2)	93.56(4)	–	–
S(1)–M(1)–S(51)	175.56(6)	–	–
S(51)–Pt(2)–S(59)	90.84(6)	–	–
P(51)–Pt(2)–P(52)	98.15(6)	–	–
P(51)–Pt(2)–S(51)	88.78(6)	–	–
P(52)–Pt(2)–S(59)	82.50(6)	–	–
P(51)–Pt(2)–S(59)	173.80(6)	–	–
P(52)–Pt(2)–S(51)	172.74(6)	–	–
Pt(2)–S(51)–C(51)	115.9(2)	–	–
Pt(2)–S(51)–M(1)	94.29(6)	–	–
C(51)–S(51)–M(1)	104.0(2)	–	–
C(59)–S(59)–Pt(2)	111.0(2)	–	–
Pt(2)–S(59)–M(2)	100.46(6)	–	–
C(59)–S(59)–M(2)	108.6(2)	–	–
S(51)–C(51)–C(60)	128.4(5)	–	–
C(60)–C(59)–S(59)	127.5(5)	–	–
C(51)–C(60)–C(59)	126.7(6)	–	–
S(9)–M(2)–M(1)	96.65(4)	–	–
S(59)–M(2)–M(1)	94.46(4)	–	–
S(9)–M(2)–S(59)	168.81(6)	–	–
Splay angle	22.4, 22.6	24.0	22.7
Dihedral angle	142, 146	149	150

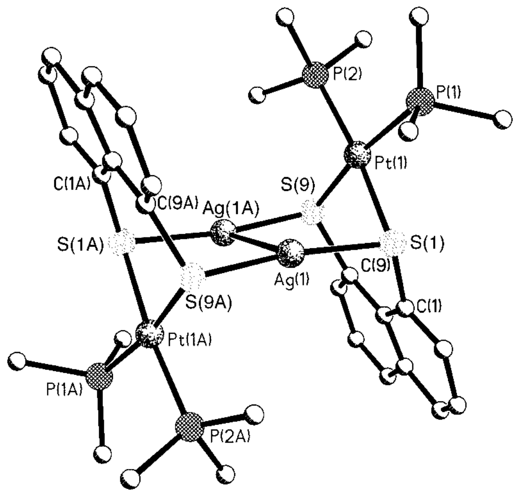

Figure 7. Crystal structure of $[Ag(Ph_3P)_2Pt(S_2C_{10}H_6)]_2^{2+}2ClO_4^-$ (**4**); ClO_4^- anions are omitted for clarity.

The metal–metal bond lengths [2.9801(4), 3.0042(14) and 3.069(4) Å] are larger than those seen in similar sulfur–platinum complexes containing a gold–gold[10] or silver–silver[13] bond, but are still short enough to confirm a metal–metal interaction. Metal–sulfur bond lengths are similar and unremarkable. The M–M–S angles are in the range 90.77(4)–95.10(10)°, and the S–M–S angles are in the range 171.28(16)–175.56(6)°. This signifies that the metal atoms are in only slightly distorted T-shaped environments. Again, these values are close to those of previously studied examples.[10,13] One major point worth mentioning is that the presence of two metal atoms in the bridge actually pushes the sulfur atoms more into the plane of the Pt and C(10) atoms, giving these structures a greater dihedral angle than in $(Me_3P)_2Pt(S_2C_{10}H_6)$, as opposed to a smaller dihedral angle in the case of complex **3**. These values now lie in the range 142–150° compared with 136° in $(Me_3P)_2Pt(S_2C_{10}H_6)$ and 121–124° in complexes **1** and **3**.

Conclusions

This paper illustrates the ability of sulfur-donor atoms to bridge metal centres. It is apparent that the planar naphthalene backbone used here is sterically undemanding with respect to. bridging systems, and thus these ligands may be capable of supporting many different multimetallic systems.

Experimental Section

General: Manipulations were performed under anoxygen-free nitrogen atmosphere using standard Schlenk techniques and glassware. Solvents were dried, purified and stored according to common procedures.[16] [Naphthalene-1,8-bis(thiolato)]bis(triphenylphenylphosphane)platinum was prepared according to literature procedures.[14] $^{31}P\{^1H\}$ (109.4 MHz) and ^{195}Pt (58.1 MHz) NMR spectra were recorded with a Jeol DELTA GSX270 spectrometer with $\delta(^{31}P)$ referenced to external 85% H_3PO_4 and $\delta(^{195}Pt)$ to external H_2PtCl_6. ES+ mass spectra were carried out by the University of St Andrews Mass Spectrometry Service.

$[(Ph_3P)_2Pt(S_2C_{10}H_6)(AuPPh_3)][ClO_4]$ (1): Ph_3PAuCl (0.049 g, 0.1 mmol) was dissolved in dichloromethane (5 cm^3), and $AgClO_4$ (0.021 g, 0.1 mmol) in acetonitrile (1 cm^3) was added. The mixture was stirred in the dark for 2 h. A white solid precipitated, which was then dried in vacuo, redissolved in dichloromethane (10 cm^3) and filtered to remove insoluble AgCl. Solid $(Ph_3P)_2Pt(S_2C_{10}H_6)$ (0.091 g, 0.1 mmol) was added in one portion, and the mixture was allowed to stir overnight. The resulting solution was filtered through celite and washed with dichloromethane (20 cm^3). The solution was reduced in volume to approximately 1 cm^3, and the final product was precipitated by slow addition of diethyl ether (15 cm^3). The final product was filtered off and dried in vacuo as a yellow powder. Yield 0.079 g, 58%. ^{31}P NMR (CD_2Cl_2): δ = 17.6 [$^1J(P_A,Pt)$ = 3080 Hz, Pt–*P*], 32.69 (Au–*P*) ppm. ^{195}Pt NMR (CD_2Cl_2): δ = –4674 ppm. ES+ MS: *m/z* = 1368 [M]+. ES– MS: *m/z* = 99 $[ClO_4]^-$.

$[Au(Ph_3P)_2Pt(S_2C_{10}H_6)]_2[ClO4]_2$ (2): Ph_3PAuCl (0.098 g, 0.2 mmol) was dissolved in dichloromethane (5 cm^3), and $AgClO_4$ (0.042 g, 0.2 mmol) in acetonitrile (1 cm^3) was added. The mixture was stirred in the dark for 2 h. A white solid precipitated, which was then dried in vacuo, redissolved in dichloromethane (10 cm^3) and filtered to remove insoluble AgCl. Solid $(Ph_3P)_2Pt(S_2C_{10}H_6)$ (0.091 g, 0.1 mmol) was added in one portion, and the mixture was allowed to stir overnight. The resulting solution was filtered through celite and washed with dichloromethane (20 cm^3). The solution was reduced in volume to approximately 1 cm^3, and the final product was precipitated by slow addition of diethyl ether (15 cm^3). The final product was filtered off and dried in vacuo as a yellow powder. Yield 0.074 g, 67%. ^{31}P NMR (CD_2Cl_2): δ = 14.4 [$^1J(P_A,Pt)$ = 3134 Hz] ppm. ^{195}Pt NMR (CD_2Cl_2): δ = –4563 ppm. ES+ MS: *m/z*= 1107 [1/2 M]+. ES– MS: *m/z* = 99 $[ClO_4]^-$.

$Ag[(Ph_3P)_2Pt(S_2C_{10}H_6)]_2[ClO_4]$ (3): $(Ph_3P)_2Pt(S_2C_{10}H_6)$ (0.150 g, 0.165 mmol) was dissolved in tetrahydrofuran (15 cm^3), and a solution of $AgClO_4$ (0.017 g, 0.0825 mmol) in acetonitrile (10 cm^3) was slowly added. The mixture was stirred for 3 h. The resulting solution was dried in vacuo, redissolved in a minimum volume of dichloromethane, and the final product was precipitated by slow addition of diethyl ether (20 cm^3). The final product was filtered off and dried in vacuo as an orange powder. Yield 0.081 g, 51%. ^{31}P NMR (CD_2Cl_2): δ = 6.83 [$^1J(P_A,Pt)$ = 2989 Hz] ppm. ^{195}Pt NMR (CD_2Cl_2): δ = –4698 ppm. ES+ MS: *m/z* = 1928 [M]+. ES– MS: *m/z* = 99 $[ClO_4]^-$.

$[Ag(Ph_3P)_2Pt(S_2C_{10}H_6)]_2[ClO_4]_2$ (4): $(Ph_3P)_2Pt(S_2C_{10}H_6)$ (0.150 g, 0.165 mmol) was dissolved in tetrahydrofuran (15 cm^3), and a solution of $AgClO_4$ (0.034 g, 0.165 mmol) in acetonitrile (10 cm^3) was slowly added. The mixture was stirred for 3 h. The resulting solution was dried in vacuo, redissolved in a minimum volume of dichloromethane, and the final product was precipitated by slow addition of diethyl ether (20 cm^3). The final product was filtered off and dried in vacuo as a yellow powder. Yield 0.101 g, 60%. ^{31}P NMR (CD_2Cl_2): δ = 18.29 [$^1J(P_A,Pt)$ = 3122 Hz] ppm. ES+ MS: *m/z* = 1928 [M]+. ES– MS: *m/z* = 99 $[ClO_4]^-$.

Crystal-Structure Analysis: Table 3 lists the details of data collections and refinements. Intensities were corrected for Lorentz-polarisation and for absorption. For **1**, **2** and **2′**, data were collected at 93 K by using Mo-K_α radiation from a high brilliance Rigaku MM007 generator and a Rigaku Mercury ccd detector, and for **3** and **4**, at 93 K using a Rigaku Saturn70 ccd detector. The structures were solved by the heavy-atom method or by direct methods. The positions of the hydrogen atoms were idealised. Refinements were performed by full-matrix least-squares based on F^2 with SHELXTL.[17] CCDC-614032–614036 for **1**–**4** contain the supple-

Table 3. Crystallographic data for complexes **1**–**4**.

	1	**2**	**2′**	**3**	**4**
Empirical formula	$C_{64}H_{51}AuClO_4P_3PtS_2$	$C_{95}H_{78}Au_2Cl_8O_8P_4Pt_2S_4$	$C_{96}H_{80}Au_2Cl_{10}O_8P_4Pt_2S_4$	$C_{92}H_{72}AgClO_4P_4Pt_2S_4$	$C_{96}H_{96}Ag_2Cl_{10}O_{16}P_4Pt_2S_4$
M	1468.58	2667.41	2752.33	2027.12	2718.27
Crystal system	orthorhombic	monoclinic	triclinic	monoclinic	triclinic
Space group	*Pbca*	*P21/n*	$P\bar{1}$	*P21/c*	$P\bar{1}$
a [Å]	24.0844(19)	17.8905(16)	12.022(2)	22.7346(15)	12.181(8)
b [Å]	18.3113(11)	14.8263(13)	13.401(3)	14.6105(9)	15.192(9)
c [Å]	25.076(2)	34.810(3)	16.917(3)	26.0999(18)	16.788(10)
α [°]	90	90	84.158(11)	90	66.82(6)
β [°]	90	95.180(2)	69.678(8)	114.872(3)	69.11(6)
γ [°]	90	90	67.000(8)	90	69.45(5)
U [Å^3]	11059.1(14)	9195.5(15)	2350.8(8)	7865.3(9)	2587(3)
Z	8	4	1	4	1
$\rho_{calcd.}$ [g cm^{-3}]	1.764	1.927	1.944	1.712	1.745
μ [mm^{-1}]	5.438	6.664	6.575	4.070	3.532
Reflections measured	69772	55134	12800	51011	15497
Independent reflections	9994	16234	7453	13973	8069
FinalR_1, wR_2 [$I>2\sigma(I)$]	0.0329, 0.0630	0.0372, 0.0771	0.0722, 0.1583	0.0827, 0.1852	0.1324, 0.3528

mentary crystallographic data for this paper. These data can be obtained free of charge from The Cambridge Crystallographic Data Centre via www.ccdc.cam.ac.uk/data_request/cif.

---

[1] R. Ugo, G. La Monica, S. Cenini, A. Segre, F. Conti, *J. Chem. Soc. A* **1971**, 522–528.

[2] B. H. Aw, K. K. Looh, H. S. O. Chan, K. L. Tan, T. S. A. Hor, *J. Chem. Soc., Dalton Trans.* **1994**, 3177–3182.

[3] H. Liu, A. L. Tan, K. F. Mok, T. C. W. Mak, A. S. Batsanov, J. A. K. Howard, T. S. A. Hor, *J. Am. Chem. Soc.* **1997**, *119*, 11006–11011.

[4] S.-W. A. Fong, J. J. Vittal, W. Henderson, T. S. A. Hor, A. G. Oliver, C. E. F. Rickard, *Chem. Commun.* **2001**, 421–422.

[5] S.-W. A. Fong, W. T. Yap, J. J. Vittal, T. S. A. Hor, W. Henderson, A. G. Oliver, C. E. F. Rickard, *J. Chem. Soc., Dalton Trans.* **2001**, 1986–2002.

[6] M. Ebihara, M. Tsuchiya, M. Yamada, K. Tokoro, T. Kawamura, *Inorg. Chim. Acta* **1995**, *231*, 35–43.

[7] Z. Li, Z.-H. Loh, K. F. Mok, T. S. A. Hor, *Inorg. Chem.* **2000**, *39*, 5299–5305.

[8] W. Bos, J. J. Bour, P. P. J. Schlebos, P. Hageman, W. P. Bosman, J. M. M. Smits, J. A. C. Van Wietmarschen, P. T. Beurskens, *Inorg. Chim. Acta* **1986**, *119*, 141–148.

[9] J. Vicente, M. T. Chicote, S. Huertas, D. Bautista, P. G. Jones, A. K. Fischer, *Inorg. Chem.* **2001**, *40*, 2051–2057; J. Vicente, M. T. Chicote, S. Huertas, P. G. Jones, *Inorg. Chem.* **2001**, *40*, 6193–6200; J. Vicente, M. T. Chicote, S. Huertas, P. G. Jones, *Inorg. Chem.* **2003**, *42*, 4268–4274; Y. D. Len, L. Y. Zhang, L. X. Shi, Z. N. Chen, *Inorg. Chem.* **2004**,*43*, 7493–7501.

[10] Z. Li, K. F. Mok, T. S. A. Hor, *J. Organomet. Chem.* **2003**, *682*, 73–78.

[11] H. Liu, A. L. Tan, C. R. Cheng, K. F. Mok, T. S. A. Hor, *Inorg. Chem.* **1997**, *36*, 2916–2918.

[12] J. Fornies, A. Martin, R. Navarro, V. Sicilia, P. Villarroya, A. G. Orpen, *J. Chem. Soc., Dalton Trans.* **1998**, 3721–3726.

[13] C. E. Bryant, T. S. A. Hor, N. D. Howells, D. M. P. Mingos, *J. Organomet. Chem.* **1983**, *256*, C15–C18.

[14] a) S. M. Aucott, H. L. Milton, S. D. Robertson, A. M. Z. Slawin, G. D. Walker, J. D. Woollins, *Chem. Eur. J.* **2004**, *10*, 1666–1676; S. M. Aucott, H. L. Milton, S. D. Robertson, A. M. Z. Slawin, J. D. Woollins, *Dalton Trans.* **2004**, 3347–3352; S. M. Aucott, P. Kilian, H. L. Milton, S. D. Robertson, A. M. Z. Slawin, J. D. Woollins, *Inorg. Chem.* **2005**, *44*, 2710–2718; S. D. Robertson, A. M. Z. Slawin, J. D. Woollins, *Polyhedron* **2006**,*25*, 823–826; b) C. J. Burchell, S. M. Aucott, H. L. Milton, A. M. Z. Slawin, J. D. Woollins, *Dalton Trans.* **2004**, 369–374; R. Jones, P. F. Kelly, D. J. Williams, J. D. Woollins, *J. Chem. Soc. Chem. Soc. Chem. Commun.* **1985**, 1325–1326; R. Jones, D. J. Williams, P. T. Wood, J. D. Woollins, *Polyhedron* **1987**, *6*, 539–542; R. Jones, P. F. Kelly, D. J. Williams, J. D. Woollins, *J. Chem. Soc., Dalton Trans.* **1988**, 803–807; J. R. Phillips, A. M. Z. Slawin, A. J. P. White, D. J. Williams, J. D. Woollins, *J. Chem. Soc., Dalton Trans.* **1995**, 2467–2468; R. Cea-Olivares, V. García-Montalvo, J. Novosad, J. D. Woollins, R. A. Toscanoa, G. Espinosa-Pérez, *Chem. Ber.* **1996**,*129*, 919–923; U. Abram, E. Schulz Lang, S. Abram, J. Wegmann, J. R. Dilworth, R. Kirmse, J. D. Woollins, *J. Chem. Soc., Dalton Trans.* **1997**, 623–630; A. M. Z. Slawin, M. B. Smith, J. D. Woollins, *J. Chem. Soc., Dalton Trans.* **1996**, 3659–3665; R. Jones, D. J. Williams, P. T. Wood, J. D. Woollins, *Polyhedron* **1989**, *8*, 91–96.

[15] J. Vicente, M. T. Chicote, P. Gonzalez-Herrero, P. G. Jones, *J. Chem. Soc., Dalton Trans.* **1994**, 3183–3187.

[16] D. D. Perrin, W. L. F. Armarego, *Purification of Laboratory Chemicals*, 3rd ed., Pergamon Press, Oxford, **1988**.

[17] *SHELXTL 6.10*, Bruker AXS, Madison.

Received: August 25, 2006
Published Online: November 13, 2006